



Fixed-Bed Column Adsorption of Copper Ions Using Activated Orange Charcoal: Performance, Thermodynamic Studies, and SEM-FTIR Characterization


Mohamed Ali Aldeib^{1*}, Ali Salem Elewan², Ziad Emhamed Brik³

^{1,2,3} Chemical engineering department, college of engineering, Alasmarya Islamic University, Zliten, Libya.
m.aldeip@asmarya.edu.ly

امتزاز أيونات النحاس باستخدام عمود الحشوة الثابتة بواسطة فحم البرتقال المنشط: الأداء، الدراسات الديناميكية الحرارية، والتوصيف بتقنيتي المجهر الإلكتروني الماسح ومطيافية الأشعة تحت الحمراء بتحويل فورير (SEM-FTIR)

محمد علي الديب^{1*}، علي سالم اعليوان²، زياد امجد بريك³

^{1,2,3} قسم الهندسة الكيميائية، كلية الهندسة، الجامعة الأسمرية الإسلامية، زليتن، ليبيا

Received: 09-04-2026	Accepted: 18-05-2026	Published: 23-05-2026
	Copyright: © 2026 by the authors. This article is an open-access article distributed under the terms and conditions of the Creative Commons Attribution (CC BY) license (https://creativecommons.org/licenses/by/4.0/).	

المخلص:

تتناول هذه الدراسة عملية امتزاز أيونات النحاس (Cu^{2+}) على فحم البرتقال المنشط كيميائياً بواسطة حمض الهيدروكلوريك (HCL) داخل عمود ذو طبقة ثابتة، مع التركيز على دراسة تأثير كل من التركيز الابتدائي، وجرعة الممتز، والرقم الهيدروجيني، ودرجة الحرارة. ولتوصيف المادة الممتازة، تم تحليل الخصائص المورفولوجية والكيميائية لفحم البرتقال المنشط باستخدام المجهر الإلكتروني الماسح (SEM) الذي أظهر بنية سطحية مسامية للغاية تشبه خلايا النحل مع حزم وعائية متطورة توفر مساحة سطحية عالية لترابط المعادن، ومطيافية الأشعة تحت الحمراء بتحويل فورير (FTIR) التي أكدت وجود مجموعات وظيفية رئيسية مثل مجموعات الهيدروكسيل والكاربوكسيل والتي تعمل كمواقع نشطة لجذب واحتواء أيونات النحاس وتثبيتها. وقد أظهرت النتائج التجريبية الرئيسية أن سعة الامتزاز القصوى (Qe) بلغت 69 ملجم/جم عند تركيز ابتدائي (ppm500) عند رقم هيدروجيني 6.5 وجرعة مثالية قدرها 0.2 جرام من الكربون المنشط، مع تسجيل أعلى كفاءة إزالة بنسبة 89% خلال 30 دقيقة فقط. ومن ناحية الحركية الحرارية، أدى رفع درجة الحرارة من 298 كلفن إلى 313 كلفن إلى تعزيز سعة الامتزاز، وسجلت المعاملات الترموديناميكية قيم إنثالبي التفاعل بلغت $\Delta H = 1.28 \text{ kJ/mol}$ ، وإنتروبي التفاعل بلغت $\Delta S = 4.29 \text{ J/mol}\cdot\text{K}$ ، وطاقة جيبس الحرة بلغت $\Delta G = 5.14 \text{ J/mol}$ مما يشير علمياً إلى أن عملية الامتزاز ماصة للحرارة وتصحباها زيادة في العشوائية عند الحد الفاصل بين الحالة الصلبة والسائلة، مع بقائها غير تلقائية تحت هذه الظروف القياسية المحددة. وفيما يتعلق بنمذجة العمود، تم تحليل بيانات اختراق العمود باستخدام نماذج (Adams-Bohart) و (Yoon-Nelson) و (Thomas) ومن بين هذه النماذج، قدم نموذج (Adams-Bohart) أفضل مطابقة ($R^2=0.91$). وتؤكد هذه النتائج، المدعومة بالرؤى المورفولوجية والكيميائية الناتجة عن تحليلي (SEM) و (FTIR)، على فاعلية فحم البرتقال المنشط بحامض الهيدروكلوريك كمتزّ مُستدام لإزالة النحاس في التطبيقات البيئية.

الكلمات الدالة: كربون البرتقال المنشط، امتزاز النحاس، عمود ذو طبقة ثابتة، توصيف وبنية (SEM-FTIR)، نماذج الاختراق.

Abstract

This study evaluates the performance of hydrochloric acid (HCl)-activated orange charcoal as a sustainable bio-based adsorbent for the removal of Cu^{2+} ions from aqueous solutions using a fixed-bed column system. The influence of key operational parameters, including initial copper concentration, adsorbent dosage, solution pH, contact time, and temperature, was systematically evaluated to optimise the adsorption process. The physicochemical properties of the prepared adsorbent were characterised using Scanning Electron Microscopy (SEM) and Fourier Transform Infrared Spectroscopy (FTIR). SEM analysis revealed a highly porous honeycomb-like morphology with well-preserved vascular channels, providing an extensive surface area and favourable pore architecture for metal ion adsorption. FTIR analysis confirmed the presence of oxygen-containing functional groups, particularly hydroxyl and carboxyl moieties, which serve as the primary active sites responsible for Cu^{2+} binding. The experimental findings demonstrated that adsorption performance was strongly influenced by the investigated operating conditions. The maximum adsorption capacity (Q_e) of 69 mg/g was achieved at an initial Cu^{2+} concentration of 500 ppm, an adsorbent dosage of 0.2 g, and an optimum solution pH of 6.5, resulting in a copper removal efficiency of approximately 89% after 30 min of contact time. Furthermore, increasing the operating temperature from 298 to 313 K enhanced the adsorption capacity, indicating that the process is thermally favourable. Thermodynamic evaluation yielded positive values of ΔH (1.28 kJ/mol) and ΔS (4.29 J/mol·K), suggesting an endothermic adsorption process accompanied by increased randomness at the solid–liquid interface. The positive Gibbs free energy ($\Delta G = 5.14$ J/mol) indicates that adsorption is non-spontaneous under the investigated standard conditions but may become more favourable at elevated temperatures. The dynamic adsorption behaviour of the fixed-bed column was successfully interpreted using the Adams–Bohart, Thomas, and Yoon–Nelson models. Among these, the Adams–Bohart model exhibited the highest predictive capability, with a coefficient of determination (R^2) of 0.91, indicating good agreement with the experimental breakthrough data. Collectively, the morphological, spectroscopic, thermodynamic, and modelling results demonstrate that HCl-activated orange charcoal is an efficient, low-cost, and environmentally sustainable adsorbent with considerable potential for the treatment of copper-contaminated wastewater and other heavy metal remediation applications.

Keywords: Activated orange charcoal, Copper adsorption, Fixed-bed column, SEM-FTIR characterization, Breakthrough models.

1. Introduction

The increasing emission of heavy metals to aquatic ecosystems has become a significant global environmental problem, mainly due to rapid industrial development and increased anthropological interventions. The list of contaminants includes Cu^{2+} as one of the most common heavy metals, which result from the discharge of industrial effluent from industries such as electroplating, mining, metallurgical processing, electronic manufacture, and construction. While copper is an important micronutrient participating in various physiological and biochemical reactions, its presence in aquatic systems at a high concentration represents an acute environmental and health risk because of its non-degradable nature, persistency, bioaccumulation, and adverse impacts on the aquatic ecosystem and human beings (Elboughdiri et al., 2024). Management of metal-contaminated wastewater from industries continues to be one of the major challenges technologically and environmentally. Various approaches such as sedimentation, flocculation, chemical coagulation, chemical precipitation, ion exchange, membrane filtration, and reverse osmosis have been widely employed to remove the contaminants. However, some limitations of these technologies include high cost, high energy consumption, production of hazardous waste, low treatment efficiency of dissolved metals, among others. Moreover, the solubility, chemical stability, and high resistance of heavy metal ions to biological degradation present major challenges when applying traditional wastewater management technologies (Mfoumou et al., 2024). Several research papers have shown that agricultural waste products such as chemically activated orange charcoal can be used as cost-efficient adsorbents in removing heavy metals. Orange charcoal is a product made from the biomass of orange tree and it is a sustainable adsorbent compared to other adsorbents because of its abundance and low cost of preparation (Aldeib et al., 2024). Through the chemical activation using hydrochloric acid HCL, the porosity and surface area of the charcoal increase, thus enabling higher adsorption rates for copper ions (Rápó & Tonk, 2021). This paper intends to examine the efficiency of chemically activated orange charcoal in adsorbing Cu^{2+} ions from aqueous solution by performing a comprehensive analysis based on different parameters such as concentration of copper ions, pH, adsorbent dose, and temperature.

2-Methodology

2.1 Materials and Equipment:

Orange charcoal used as the adsorbent precursor was procured from local markets in Libya. Concentrated hydrochloric acid (HCl) was employed as the chemical activating agent to modify the surface characteristics of the charcoal. Copper nitrate trihydrate ($\text{Cu}(\text{NO}_3)_2 \cdot 3\text{H}_2\text{O}$) served as the source of Cu^{2+} ions for the preparation of aqueous copper solutions. All adsorption experiments were conducted using a laboratory-scale fixed-bed column fabricated from either glass or acrylic material. The chemicals used in this study were of analytical grade and were utilised without further purification. Additional equipment includes pumps for controlling the flow rate, a flow meter, a pH meter, filtration setup for effluent collection, and a spectrophotometer for concentration analysis.

2.2 Preparation of Activated Carbon

The orange charcoal was obtained from local markets in Libya. It was then washed with distilled water to remove impurities and dust. After that, it was dried in sunlight and then in a drying oven at a temperature of 105°C for several hours. It was then crushed into small pieces and soaked in hydrochloric acid at a ratio of 1:3 for 24 hours. (Alhaslook, 2023) After that, the charcoal was washed with distilled water until the charcoal washing water reached a neutral pH of 7.

2.3 Preparation of Copper Ion Solution

A stock solution of Cu (II) was prepared by dissolving copper nitrate ($\text{Cu}(\text{NO}_3)_2 \cdot 3\text{H}_2\text{O}$) in distilled water to achieve a concentration of 1000 mg/L (Hasfalina et al., 2012). Precision working solutions were then created by diluting the stock to specific concentrations of 100, 200, 300, 400, 500, 600, and 700 mg/L. The concentrations of Cu (II) in these solutions were analyzed using a spectrophotometer at an appropriate wavelength (820 nm). while the pH was measured with a pH meter to ensure optimal conditions for the adsorption process.

2.4 Fixed Bed Column Setup

A laboratory-scale transparent plastic column with a length of 10 cm and an internal diameter of 3 cm was used as the fixed-bed adsorption column. A layer of cotton wool was placed at the base of the column to support the adsorbent bed and prevent the loss of activated charcoal during the adsorption process. The column was packed with hydrochloric acid-activated orange charcoal at varying masses ranging from 0.2 to 1.0 g. Subsequently, the prepared copper ion solution was introduced into the column under gravity-driven flow, allowing continuous contact between the solution and the adsorbent bed throughout the adsorption experiment. (Nwabanne & Igbokwe, 2012), Additionally, the effects of varying pH levels from 2 to 9 concentration from 100 to 700 mg/L, and temperatures from 25 to 40 degrees Celsius were examined, alongside the varying amounts of adsorbent used.

3. Thermodynamic studies

Thermodynamic parameters like Gibbs free energy (ΔG° , J/mol), entropy (ΔS° , J/mol·K), and enthalpy (ΔH° , J/mol) were utilized to characterize the thermodynamic behavior of the adsorbent. These parameters were calculated using specific mathematical equations.

$$\Delta G^\circ = -RT \ln kd \quad (1)$$

$$kd = (\text{Co} - \text{Ce}) / \text{Ce} \times V/m \quad (2)$$

$$\ln kd = \Delta S^\circ / R - \Delta H^\circ / RT \quad (3)$$

In this context, $\ln kd$ (L/g) refers to the distribution coefficient, T (K) indicates the absolute temperature, and R (J/mol·K) represents the universal gas constant. (Mokokwe & Letshwenyo, 2022).

3.1 performance fixed bed column

3.1.1 Thomas Model

The Thomas model is commonly used to calculate the adsorption capacity of an adsorbent and to predict the breakthrough curve. It is based on the assumption of second-order reversible reaction kinetics and follows the Langmuir isotherm. (Han.,2008 & Ghasemi.,2011). The linear form of the Thomas model can be expressed as:

$$\ln [(C_0 / C_t) - 1] = K_{TH} q_0 M / Q - K_{TH} C_0 t \quad (4)$$

Where:

- C_0 : Initial concentration of copper ions (mg/L)
- C_t : Effluent concentration of copper ions at time t (mg/L)
- K_{TH} : Thomas model constant (L/min·mg)
- q_0 : Predicted adsorption capacity (mg/g)
- M : Mass of the adsorbent (g)
- Q : Inlet flow rate (mL/min), The value of K_{TH} and q_0 are determined from slope and intercept of a plot of $\ln [(C_0/C_t - 1)]$ versus t.

3.1.2 Yoon - Nelson Model

The primary objective of the Yoon-Nelson model is to estimate the operational duration of a column before regeneration becomes necessary. This model specifically predicts that the amount of Cu^{+2} adsorbed in a packed bed reaches half of the total Cu^{+2} entering the adsorbent bed within a time span of $\tau/2$, where τ is the time required to achieve 50% breakthrough. (Rouf & Nagapadma.,2015)

$$\ln [C_t / (C_0 - C_t)] = K_{YN} t - \tau K_{YN} \quad (5)$$

In the context of the Yoon-Nelson model, the following parameters are defined:

C_0 : Initial copper ions concentration (mg/L), C_t : copper ions concentration at time t (mg/L), t: Flow time (min), τ : Time required for 50% breakthrough (min), K_{YN} : Yoon-Nelson rate constant (L/min), Determining Constants, The values of K_{YN} and τ can be obtained from the slope and intercept of the plot of $\ln [C_t / (C_0 - C_t)]$ versus t, Adsorption Capacity Calculation, The adsorption capacity (q_e) in mg/g can be calculated using the following equation (Rocha et al .,2015).

$$q_e = C_0 Q \tau / m \quad (6)$$

Where:

- C_0 = Initial copper ions concentration (mg/L)
- Q = Inlet flow rate (mL/min)
- τ = Time required for 50% breakthrough (min)
- m = Mass of adsorbents (g)

This equation allows for the estimation of the adsorbent's capacity to remove copper ions from the solution in a packed bed column.

3.1.3 Adams-Bohart Model

The Adams-Bohart model is utilized to describe the initial phase of the breakthrough curve. It highlights that during this phase, the kinetics of adsorption are primarily influenced by external mass transfer. This model is founded on the

principle that the rate of adsorption is proportional to both the remaining capacity of the adsorbent and the concentration of the solute.(Talib .,2018)

$$\ln (C_t/C_o)= k_{AB}C_o t - [(k_{AB}N_o Z)/v] \quad (7)$$

In the Adams-Bohart model, the following parameters are defined:

- C_o : Inlet concentration of copper ions (mg/L)
- C_t : Outlet concentration of phenol (mg/L)
- k_{AB} : Kinetic constant (L·mg/min)
- v : Linear velocity of the fluid (cm/min)
- Z : Length of the adsorbent bed (cm)
- N_o : Saturation concentration of the adsorbent (mg/L)

Determining Constants:The values of k_{AB} and N_o can be obtained from the slope and intercept of the linear plot of $\ln (C_t/C_o)$ against time t .

This equation offers valuable insights into the adsorption process, aiding in the prediction of the performance of the adsorption column.

4. Results and discussion

4.1 Effect of initial concentration.

Figure 4.1 demonstrates the adsorption behaviour of Cu^{2+} ions onto activated orange charcoal at initial concentrations ranging from 100 to 700 ppm. The results illustrate the relationship between the initial copper concentration and the equilibrium adsorption capacity (Q_e). Overall, Q_e increases progressively as the concentration rises from 100 to 500 ppm, reaching a maximum value of 44.4 mg/g at 500 ppm. This trend indicates that higher solute availability enhances the driving force for mass transfer, thereby promoting more effective interaction between copper ions and the active sites of the adsorbent. Beyond the optimum concentration, the adsorption capacity tends to plateau, suggesting that the available active sites on the charcoal surface become increasingly occupied and approach saturation. At higher concentrations, a slight decline or stabilization in Q_e may be observed, which can be attributed to competition among excess Cu^{2+} ions for the limited number of remaining adsorption sites. This behaviour reflects the finite adsorption capacity of the activated orange charcoal and highlights the saturation limit of the system under the studied conditions.

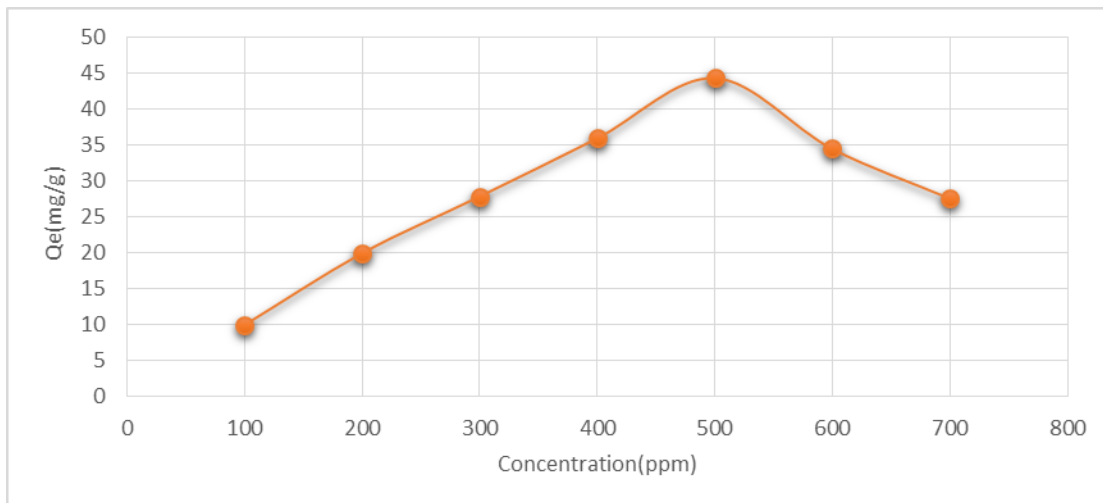


Figure 4.1: Adsorption Capacity of Copper Ions onto Activated Orange Charcoal at Varying Concentrations

4.2 Effect of time on the adsorption process.

Figure 2 illustrates the influence of contact time on the removal efficiency of Cu^{2+} ions using HCl-activated orange charcoal. At the initial stage of the process, a rapid decline in copper concentration is observed, with a removal

efficiency of 26% achieved within the first 5 minutes. This sharp initial uptake reflects the abundance of available active sites on the adsorbent surface and the strong driving force for mass transfer during the early stages of adsorption. As contact time increases, the removal efficiency continues to rise, reaching 51.85% after 10 minutes and 59.26% after 20 minutes. This gradual increase indicates sustained adsorption as more Cu^{2+} ions diffuse from the bulk solution to the surface of the activated charcoal. After 30 minutes, the removal efficiency significantly improves to 88.8% and subsequently remains nearly constant up to 40 minutes. The observed plateau suggests that adsorption equilibrium has been reached, where most of the active sites on the charcoal surface are occupied and the rate of adsorption is balanced by the rate of desorption. Beyond this equilibrium point, no substantial improvement in removal efficiency is observed. Overall, the results demonstrate that increasing contact time enhances copper ion removal until the adsorption system becomes saturated and equilibrium conditions are established.

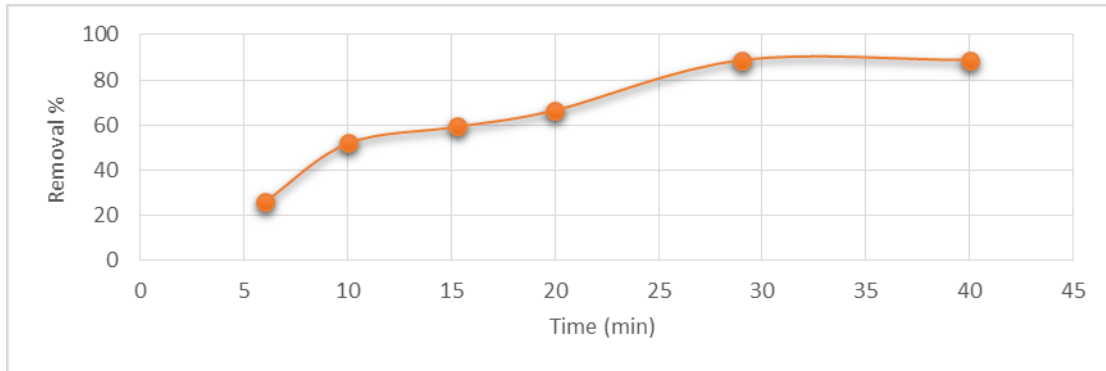


Figure 4-2: Effect of Time on the Removal of Copper Ions Using HCl-Activated Orange Charcoal

4.3 Effect of dosage

Figure 4.3 illustrates the relationship between activated orange charcoal dosage and the equilibrium adsorption capacity (Q_e) for Cu^{2+} ions. The results indicate an inverse relationship between adsorbent dose and adsorption capacity. As the dosage increases from 0.2 g to 1.0 g, Q_e decreases progressively from 68.65 mg/g to 25 mg/g, with the highest adsorption capacity recorded at the lowest dosage (0.2 g). At intermediate dosages, the adsorption capacity declines to 50.9 mg/g at 0.4 g and further to 44 mg/g at 0.6 g, suggesting a reduction in the amount of copper ions adsorbed per unit mass of adsorbent. This trend can be attributed to the increased availability of adsorption sites at higher dosages, which are not fully utilized due to the fixed amount of copper ions present in the solution, leading to a decrease in adsorption efficiency per gram of adsorbent. In addition, possible particle aggregation at higher dosages may reduce the effective surface area available for metal binding. At the highest investigated dosage (1.0 g), the adsorption capacity reaches its minimum value of 25 mg/g, indicating that excessive adsorbent addition does not enhance, and may even dilute, the adsorption efficiency on a per-mass basis. Overall, the results suggest that there is an optimum operational window for adsorbent dosage, where efficient utilization of active sites is achieved. Based on the experimental findings, the optimal conditions for copper removal were identified as an initial concentration of 500 ppm, a contact time of 30 minutes, and a moderate adsorbent dosage range that ensures effective utilization of adsorption sites.

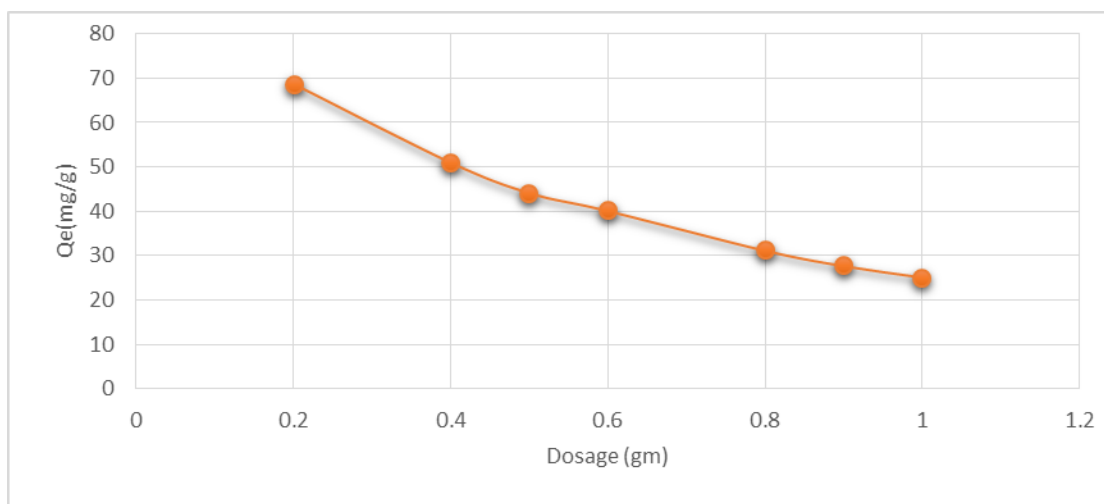


Figure 4-3: Effect of Dosage on the Adsorption Capacity of Copper Ions Using Activated Orange Charcoal

4.4 Effect of pH

Figure 4.4 demonstrates the influence of solution pH on the removal efficiency of Cu^{2+} ions using activated orange charcoal. The results reveal a strong dependence of adsorption performance on pH, where the removal efficiency increases progressively as the pH rises from 2 to approximately 6.5. The maximum removal efficiency of 85.7% is achieved at pH 6.5, indicating this value as the optimal condition for copper adsorption. At strongly acidic conditions ($\text{pH} < 7$), the reduction in removal efficiency can be attributed to the high concentration of H^+ ions in solution, which compete with Cu^{2+} ions for the available active adsorption sites on the charcoal surface. This competition significantly suppresses the uptake of copper ions. In contrast, at alkaline conditions (pH 9), the removal efficiency decreases markedly to 38.6%, which may be associated with the formation of insoluble copper hydroxide species, leading to a reduction in the concentration of free Cu^{2+} ions available for adsorption. Overall, the findings highlight that pH plays a critical role in governing the surface chemistry of the adsorbent as well as the speciation of copper ions, thereby directly influencing the overall adsorption performance.

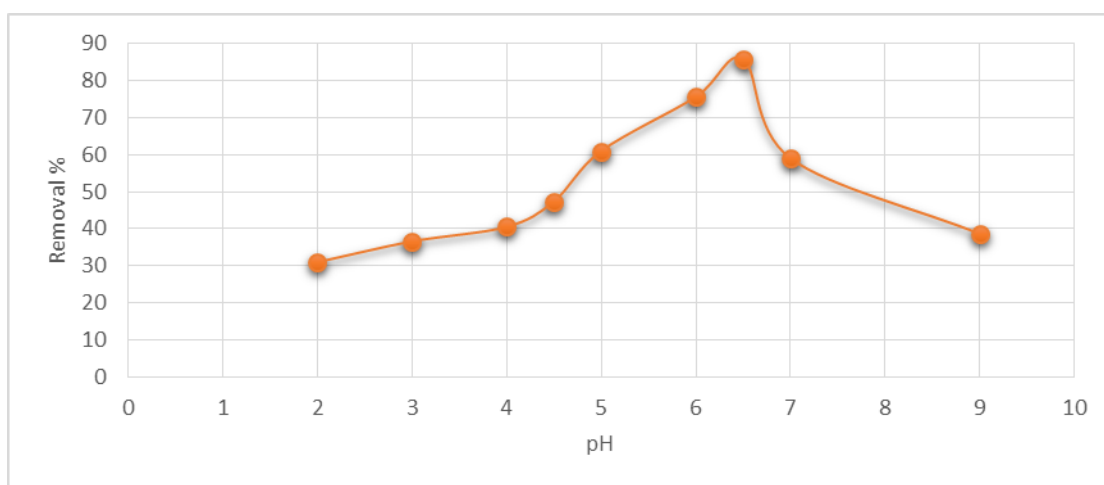


Figure 4.4: Effect of pH on Copper Ion Adsorption through Adsorption

4.5 Effect of temperature

Figures 4.5 and 4.6 show that as the temperature increases from 298 K to 313 K, the adsorption capacity of copper ions on chemically activated orange charcoal reaches a maximum of 58 mg/g at 40 °C (313 K). This increase is due to enhanced molecular activity and higher kinetic energy, leading to more effective collisions at the adsorption sites. Thus, elevated temperatures positively impact the adsorption capacity.

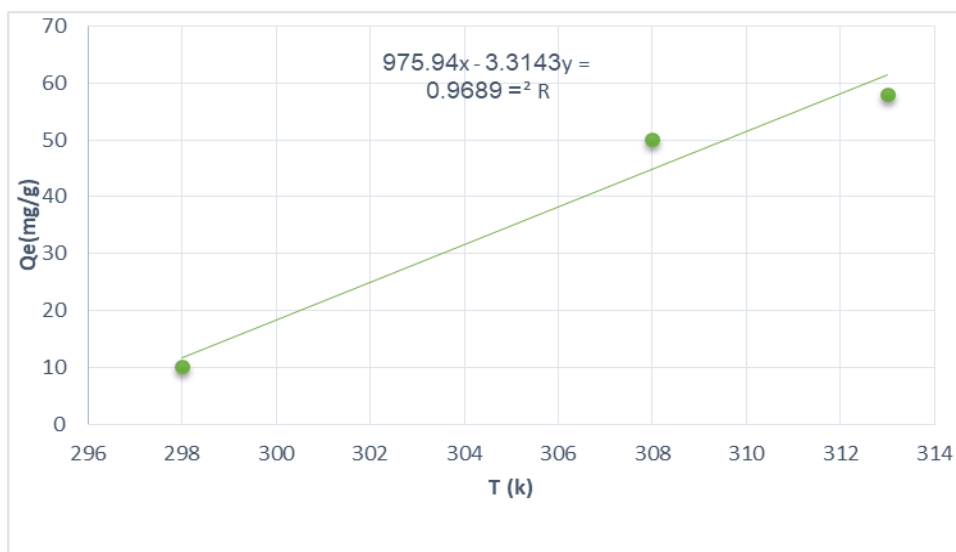


Figure 4.5 Effect of Temperature on the Adsorption Capacity of Copper Ions

From figure 4.6 and by using equation 1,2,and 3

ΔH : 1.28 kJ/mol

ΔS : 4.29 J/mol·K

ΔG : 5.14 J/mol (or approximately 0.00514 kJ/mol)

The thermodynamic analysis reveals a positive enthalpy change ($\Delta H = 1.28$ kJ/mol), indicating that the adsorption process is endothermic in nature and proceeds with heat uptake from the surrounding environment. The positive entropy change ($\Delta S = 4.29$ J/mol·K) suggests an increase in randomness at the solid–solution interface, implying that the system becomes more disordered upon adsorption, which can potentially enhance the driving force of the process under suitable conditions. In contrast, the positive Gibbs free energy change ($\Delta G = 5.14$ J/mol) indicates that the process is non-spontaneous under standard conditions and requires an external energy input to proceed. Despite this, the thermodynamic profile suggests that the adsorption may become more favourable at elevated temperatures, where the contribution of entropy becomes more significant in overcoming the positive enthalpy barrier. Overall, the combined thermodynamic parameters highlight a temperature-dependent process, where adsorption performance is governed by the interplay between enthalpy, entropy, and Gibbs free energy, providing valuable insight into the energetic feasibility and mechanism of the system.

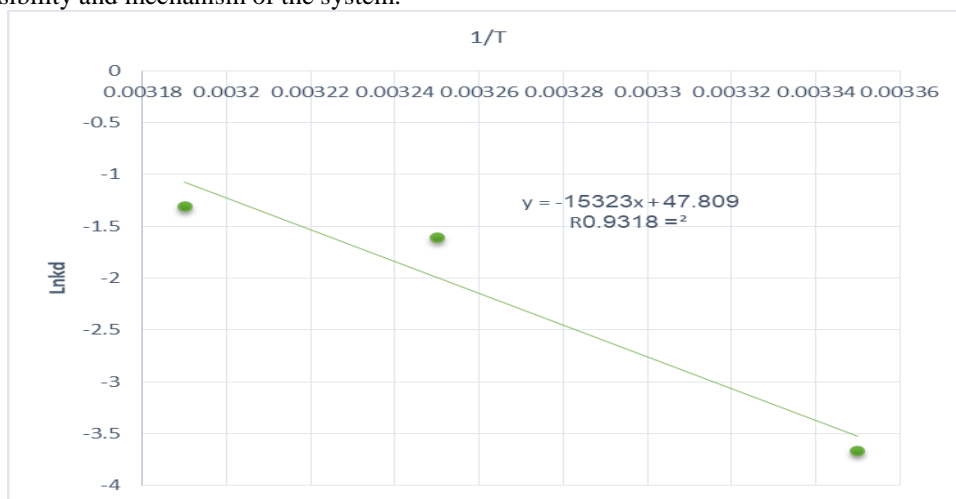


Figure 4.6 Arrhenius Plot of $\ln(k_d)$ against $1/T$

4.6 kinetics and equilibrium of the adsorption process

Figure 4.7 presents the Thomas model fitting, which describes the fixed-bed adsorption behaviour of chemically activated carbon toward Cu^{2+} ions. The obtained results demonstrate a satisfactory correlation between the experimental data and the model predictions, indicating that the Thomas model effectively represents the adsorption performance and confirms the considerable capacity of the adsorbent for copper removal. The corresponding breakthrough curve exhibits a characteristic profile, with an initial steep adsorption phase followed by a gradual approach to saturation. This behaviour reflects the progressive occupation of available active sites and the dynamic equilibrium established between Cu^{2+} ions in the solution and the functional groups on the carbon surface. Overall, the model highlights the efficiency of the adsorption process under continuous flow conditions and provides useful insight into the mass transfer and column performance characteristics.

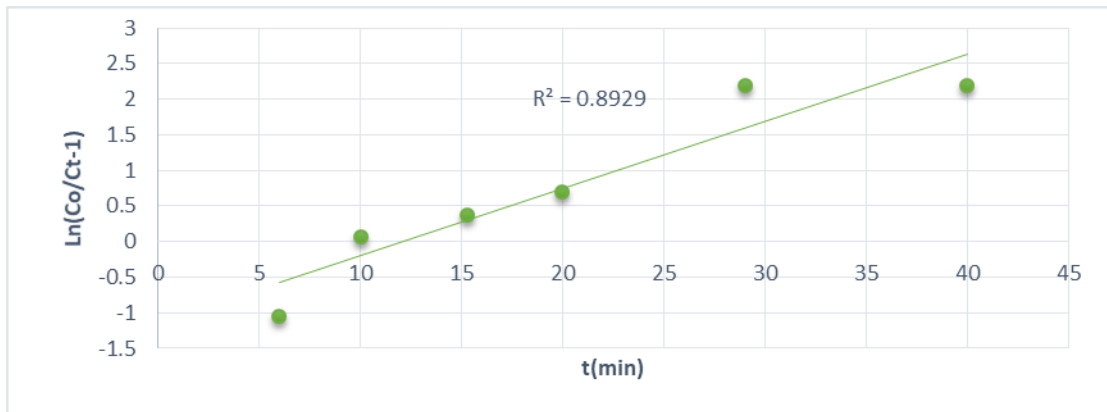


Figure 4.7 Thomas Model for Adsorption

Figure 4.8 illustrates the Yoon-Nelson model, which focuses on the kinetics of copper ion adsorption onto activated carbon. Results indicate that the rate of adsorption decreases over time, suggesting a reduction in available active sites as saturation is approached. This model aids in determining the optimal contact time for effective ion removal

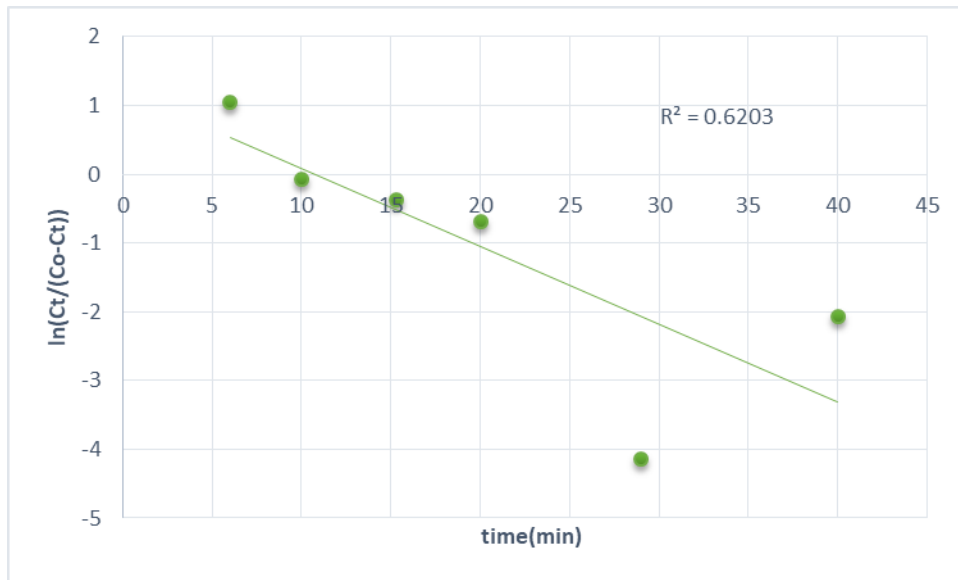


Figure 4.8 Yoon-Nelson Model for Adsorption Kinetics

Figure 4.9 presents the Adams–Bohart model, which is widely used to describe the initial mass transfer behaviour in fixed-bed adsorption systems. The results generally indicate a distinct shift from an initial rapid adsorption stage to a progressively slower uptake phase as the column approaches saturation and equilibrium conditions are established. This model is particularly valuable for interpreting the early breakthrough region and for evaluating the influence of operational parameters such as flow rate and bed height on column performance. Overall, it provides important

insights into the kinetics of the adsorption front and the efficiency of copper ion removal under dynamic operating conditions.

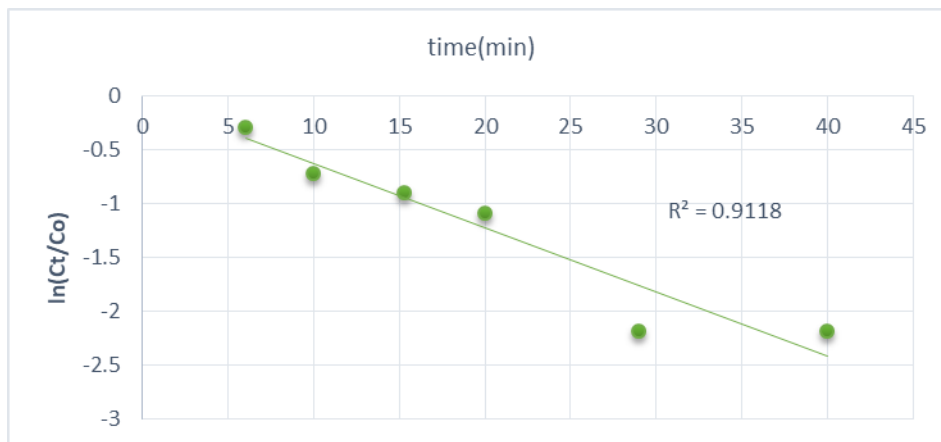


Figure 4.9 Adams-Bohart Model

Figure 4.10 presents the FTIR spectrum of hydrochloric acid (HCl)-activated orange charcoal, revealing a range of characteristic absorption bands associated with diverse surface functional groups that contribute to its enhanced adsorption performance. A broad and intense band observed in the region of 3300–3600 cm^{-1} is attributed to O–H stretching vibrations originating from hydroxyl groups, including phenolic, alcoholic, and carboxylic species. The presence of these functional groups indicates strong hydrophilic character and a high affinity for polar adsorbates, which is beneficial for metal ion uptake. Additional weak signals above 3600 cm^{-1} (3842.20, 3805.55, 3678.25, and 3653.18 cm^{-1}) are associated with atmospheric water vapour, representing rotational–vibrational transitions of adsorbed H_2O molecules that are commonly observed in FTIR measurements of porous materials. A distinct absorption peak at 2362.80 cm^{-1} corresponds to CO_2 stretching vibrations, likely arising from atmospheric carbon dioxide adsorbed on the material surface. In the carbonyl region, the band at 1687.71 cm^{-1} is assigned to C=O stretching vibrations associated with aldehyde, ketone, or carboxylic functional groups, while the prominent peak at 1620.21 cm^{-1} is attributed to aromatic C=C stretching, confirming the preservation of the carbonaceous skeletal structure of the activated material. Furthermore, the band at 1317.38 cm^{-1} is associated with C–O stretching vibrations of carboxylic acids and alcohol groups, indicating that acid activation either preserved or introduced oxygen-containing functionalities onto the carbon surface. In the fingerprint region, the peaks at 883.40 cm^{-1} and 781.17 cm^{-1} correspond to out-of-plane C–H bending vibrations of substituted aromatic rings, reflecting the structural characteristics of the aromatic framework. Overall, the FTIR analysis confirms that HCl activation produces a surface rich in hydroxyl, carbonyl, and carboxyl functional groups. This demonstrates that acid treatment effectively enhances surface chemistry by removing impurities and increasing the availability of active sites, thereby improving the adsorption potential of the orange charcoal for heavy metal removal.

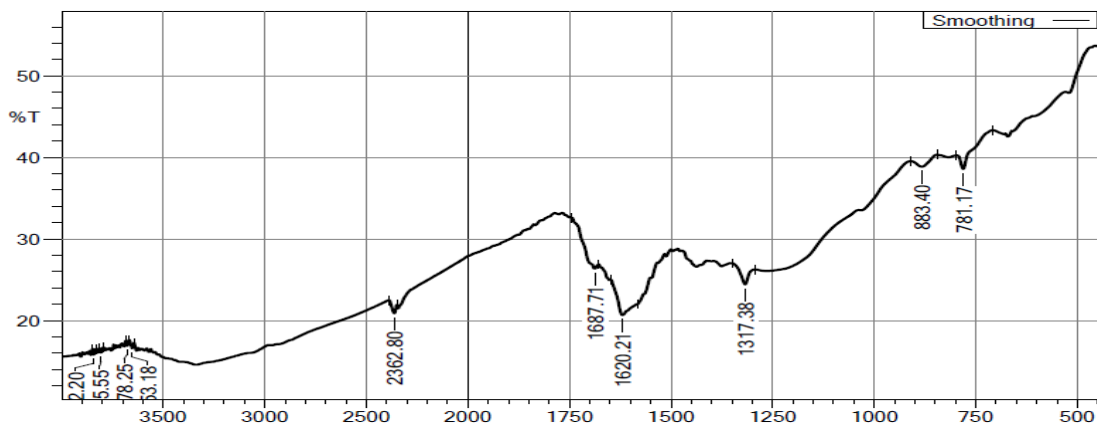


Figure 4.10. FTIR spectrum of HCl-activated orange charcoal

Figure 4.11 presents a Scanning Electron Microscopy (SEM) image of hydrochloric acid (HCl)-activated orange charcoal, offering detailed insight into its surface morphology and pore architecture at a magnification of $\times 1,000$. The micrograph reveals a well-developed, interconnected network of honeycomb-like porous structures, which is attributed to the chemical activation process. During activation, hydrochloric acid facilitates the removal of organic impurities and promotes dehydration and etching of the precursor material, leading to the formation of an extensively porous carbon framework. Distinct longitudinal channels and circular pore openings are clearly visible, reflecting the preservation of the original biological microstructure of the orange biomass, particularly the vascular bundle system (xylem and phloem). While the intrinsic anatomical features are retained, the activation process significantly enlarges the pore dimensions and enhances overall surface exposure. In addition, the surface exhibits a rough, irregular, and fragmented morphology, which is advantageous for adsorption as it increases the number of accessible active sites available for pollutant interaction. The role of HCl is pivotal in this transformation, as it removes inorganic constituents, unblocks naturally existing pores, and contributes to the development of a heterogeneous micro- and mesoporous structure. This treatment effectively converts the relatively smooth precursor surface into a highly porous, sponge-like architecture, thereby substantially increasing the Brunauer–Emmett–Teller (BET) surface area and improving adsorption efficiency for environmental applications such as water purification and gas separation. Overall, the SEM analysis (recorded at 10.0 kV with a 50.0 μm scale bar) confirms the formation of a highly porous material characterized by well-defined cylindrical channels and a honeycomb-like pore network, which is essential for its enhanced adsorption performance.



Figure 4.11. SEM micrograph of HCl-activated orange charcoal

5 Conclusion

This study demonstrates that hydrochloric acid (HCl)-activated orange charcoal represents an efficient and environmentally sustainable adsorbent for the removal of Cu^{2+} ions in a fixed-bed column system. Structural and surface characterisation using SEM and FTIR analyses confirmed the development of a highly porous, honeycomb-like architecture together with the presence of abundant oxygen-containing functional groups, both of which contribute significantly to the availability of active binding sites for metal ion adsorption. The performance of the continuous-flow adsorption process was found to be strongly influenced by key operational parameters, including initial metal ion concentration, adsorbent dosage, solution pH, and temperature. The process exhibited endothermic behaviour, indicating improved adsorption efficiency at elevated temperatures. Furthermore, the dynamic behaviour

of the column was successfully described using established kinetic and breakthrough models, confirming the reliability and predictive capability of the system. Overall, the findings highlight the potential of this low-cost, bio-derived adsorbent as a promising alternative for industrial wastewater treatment and heavy metal remediation applications.

Acknowledgements

The authors express their sincere appreciation to the Center for Nanoscience and Nanotechnology, Institute Technology Bandung, for their technical support in conducting the SEM (SU3500) analysis. Gratitude is also extended to the Laboratory of Basic Physicochemical Analysis, Faculty of Pharmacy, University of Padjadjaran, for their assistance with FTIR spectroscopic measurements. The expertise, facilities, and technical contributions of both institutions were essential to the successful completion of this research work.

References

- 1.Elboughdiri, N., Ferkous, H., Rouibah, K., Boublia, A., Delimi, A., Yadav, K. K., & Benguerba, Y. (2024). Comprehensive investigation of Cu²⁺ adsorption from wastewater using olive-waste-derived adsorbents: experimental and molecular insights. *International Journal of Molecular Sciences*, 25(2), 1028.
- 2.Mfoumou, C. M., Tonda-Mikiéla, P., Ngoye, F., Mouguala, S. B., Mbouiti, B. L., & Tchouya, G. R. F. (2024). Removal and adsorption kinetics of copper (II) ions from aqueous media on activated carbon in dynamic adsorption on a fixed-bed column. *Comptes Rendus. Chimie*, 27(G1), 141-151.
- 3.Aldeib, M. A., Bareeni, M. F., & Deab, M. H. A. (2024). Utilizing orange charcoal from citrus biomass for effective methylthioninium chloride dye removal. *North African Journal of Scientific Publishing (NAJSP)*, 22-32.
- 4.Rápó, E., & Tonk, S. (2021). Factors affecting synthetic dye adsorption; desorption studies: a review of results from the last five years (2017–2021). *Molecules*, 26(17), 5419.
- 5.Alhaslook, S. A., Aldeib, M. A., & Algesh, N. S. (2023). Assessing the viability of orange charcoal as an adsorbent for the removal of methyl orange dye from aqueous solutions. *Annual Scientific Conference for Undergraduate and Graduate Students*, 1, 6-95.
- 6.Hasfalina, C. M., Maryam, R. Z., Luqman, C. A., & Rashid, M. (2012). Adsorption of copper (II) from aqueous medium in fixed-bed column by kenaf fibres. *APCBEE Procedia*, 3, 255-263.
- 7.Nwabanne, J. T., & Igbokwe, P. K. (2012). Breakthrough curve studies for the removal of heavy metals in a fixed bed column. *Canadian Journal of Pure and Applied Sciences*, 2009.
- 8.Mokokwe, G., & Letshwenyo, M. W. (2022). Investigation of clay brick waste for the removal of copper, nickel, and iron from aqueous solution: batch and fixed-bed column studies. *Heliyon*, 8(7).
- 9.Benabid, S., Streit, A. F., Benguerba, Y., Dotto, G. L., Erto, A., & Ernst, B. (2019). Molecular modeling of anionic and cationic dyes adsorption on sludge-derived activated carbon. *Journal of Molecular Liquids*, 289, 111119.
- 10.Han, R., Ding, D., Xu, Y., Zou, W., Wang, Y., Li, Y., & Zou, L. (2008). Use of rice husk for the adsorption of Congo red from aqueous solution in column mode. *Bioresource Technology*, 99(8), 2938-2946.
- 11.Ghasemi, M., Keshtkar, A. R., Dabbagh, R., & Safdari, S. J. (2011). Biosorption of uranium (VI) from aqueous solutions by Ca-pretreated *Cystoseira indica* alga: breakthrough curves studies and modeling. *Journal of Hazardous Materials*, 189(1-2), 141-149.
- 12.Rouf, S., & Nagapadma, M. (2015). Modeling of fixed bed column studies for adsorption of azo dye on chitosan impregnated with a cationic surfactant. *International Journal of Scientific and Engineering Research*, 6(2), 124-132.
- 13.Rocha, P. D., Franca, A. S., & Oliveira, L. S. (2015). Batch and column studies of phenol adsorption by an activated carbon based on acid treatment of corn cobs. *International Journal of Engineering and Technology*, 7(6), 459.
- 14.Talib, M. I., Chauhan, Y. P., & Parate, V. R. (2018). Packed bed adsorption study on phenol removal and its modeling. In *Advance Materials, Textiles and Processes (ICAMTP-2018) Conference Paper Presented in January*.

Disclaimer/Publisher's Note: The statements, opinions, and data contained in all publications are solely those of the individual author(s) and contributor(s) and not of **JLABW** and/or the editor(s). **JLABW** and/or the editor(s) disclaim responsibility for any injury to people or property resulting from any ideas, methods, instructions, or products referred to in the content.